Observer-based fault diagnosis for trucks belt tensioner

Donatien Dubuc [*,**] **Olivier Sename** [**]
Delphine Bresch-Pietri [**] **Christophe Gauthier** [*]

[*] *Volvo Trucks, Saint Priest, France*
(e-mail: donatien.dubuc, christophe.gauthier@volvo.com)
[**] *Univ. Grenoble Alpes, CNRS, GIPSA-lab, F-38000 Grenoble, France*
(e-mail: olivier.sename, delphine.bresch-pietri@gipsa-lab.fr)

Abstract: This paper deals with the monitoring of a serpentine belt tensioner performance, a critical automotive engine component guaranteeing the cooling system efficiency. A belt tensioner fault will affect the transmission, deteriorate the water pump efficiency, and eventually, lead the engine to stall. Monitoring this component is thus a key to design predictive or corrective maintenance. In this paper, we propose to estimate a parameter which is shown to be characteristic of this component's health by using an Adaptive Observer or an Extended Kalman Filter. Respective merits of these solutions are compared using simulations performed with GT-SUITE on a high-fidelity model.

Keywords: Diagnosis, automotive systems, modeling, nonlinear observers

1. INTRODUCTION

In trucks, multiple peripheral devices such as alternator, water pump or air conditioning compressor are driven by a common belt. This belt, connected to the engine shaft, transmits the necessary mechanical power to all components in line. During the installation, the adjustment of a belt tensioner permits to hold a predetermined amount of tension on the belt, which enables it to fulfill its role.

In case of under-tension, the belt will slip, causing noise and premature wear. More importantly, it will also degrade the operation of all driven components to a subnominal state. Among others, the water pump located in the cooling system will not provide the proper coolant flow rate to the engine. This could lead the engine to overheat and, eventually, stall.

To overcome such problems, this paper proposes to estimate a parameter which is shown to be characteristic of the belt tensioner's health, via an analysis of the cooling system. The first contribution of the paper is to develop a simplified model of the cooling system for diagnosis. As common in the vehicle industry, a model-based approach has been chosen. To estimate the belt tensioner characteristic parameter, two observers have been designed and compared: an Adaptive Observer (AO) and an Extended Kalman Filter (EKF).

Among fault detection strategies (Hwang et al., 2010), the observer-based approach is a popular approach (Chen and Patton, 1999; Ding, 2008) since it introduces analytical redundancy, by estimating unknown parameters or unmeasured state variables from measurements.

The first designed observer is an AO, (Zhang and Clavel, 2001; Besançon et al., 2006) which both estimates an unknown vector parameters and the system states. It has been shown to be effective in several applicative contexts, such as for a permanent magnet synchronous motor in (Tami et al., 2014) or for the degradation of a heat exchanger in (Astorga-Zaragoza et al., 2008). The second one, the EKF, is one of the most used nonlinear observers (see (Chui and Chen, 2009) where theoretical and practical case studies are detailed). Comparison of these two well-known observer-based methods using simulation on a high-fidelity model of the cooling system are then performed. This is the second contribution of this paper.

The paper is organized as follow. In Section 2, a simplified model of the cooling system is presented. In Section 3, based on this model, an Adaptive Observer and an Extended Kalman Filter are designed to monitor the performance of the belt tensioner. Then in Section 4 we analyze the performance of the developed solutions. Finally, conclusions are stated in Section 5.

2. COOLING SYSTEM MODELING

A schematic representation of the heat exchanges involving the engine block is depicted in Fig. 1(a). To protect the different components from overheating and to ensure a good lubrication, the water pump provides the coolant flow rate necessary to remove the heat produced by the combustion.

The next section presents a simplified thermal model that will be used to design observers.

2.1 Thermal modeling of the engine block

To design a control-oriented model, a lumped-parameter approach is followed in the sequel, neglecting the distributed nature of the temperature of the coolant when flowing through the engine block. In details, we follow

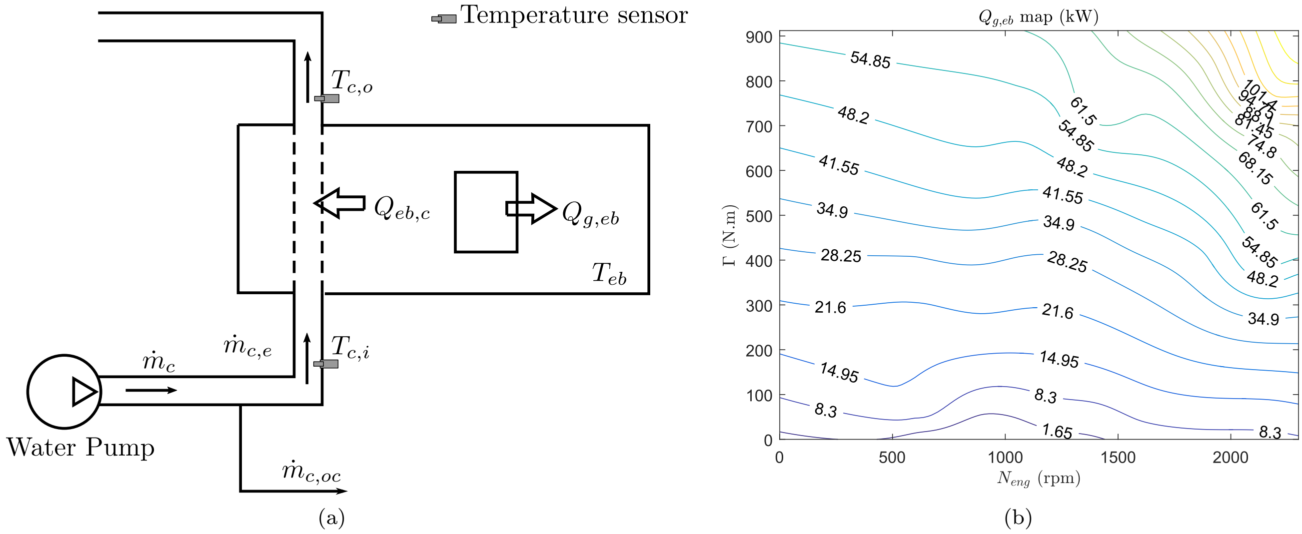

Fig. 1. (a) Flows and temperatures of the engine block (b) Heat flow from the gas to the engine block

Table 1. Nomenclature

Notation	Description	Unit
N_{eng}	Engine speed	rpm
N_{pump}	Pump speed	rpm
Γ	Engine torque	N.m
$Q_{g,eb}$	Heat flow from gas in the cylinder to the engine block	W
$Q_{eb,c}$	Heat flow from the engine block to the coolant	W
A_{eb}	Heat transfer surface area inside the engine block	m^2
T_{eb}	Temperature of the engine block	K
$T_{c,\{i,o\}}$	Coolant temperature at the inlet and at the outlet	K
h_c	Coolant heat transfer coefficient	$\text{W.m}^{-2}.\text{K}^{-1}$
c_{eb}	Heat capacity of the engine block	$\text{J.kg}^{-1}.\text{K}^{-1}$
c_c	Heat capacity of the coolant	$\text{J.kg}^{-1}.\text{K}^{-1}$
$\dot{m}_c$	Mass flow rate of the coolant	kg.s^{-1}
$\dot{m}_{c,\{e,oc\}}$	Mass flow rate of the coolant through the engine and the oil cooler	kg.s^{-1}
$m_{\{eb,c\}}$	Mass of the engine block and of the coolant in contact with the engine block	kg

a procedure similar to (Cortona et al., 2002; Astorga-Zaragoza et al., 2008; Isermann, 2014) where mean-value models are obtained from energy balances.

Let us consider the system presented in Fig. 1(a). It consists in two thermal subsystems: the engine block and the coolant.

Engine block thermal balance. A heat balance on the engine block gives the following temperature evolution:

$$\dot{T}_{eb} = \frac{Q_{g,eb} - Q_{eb,c}}{m_{eb}c_{eb}} \tag{1}$$

Note that the heat flow $Q_{g,eb}$ can be considered as an input of the model. Indeed, this flow depends on the engine operating point and its value can be obtained from a three-dimensional map (cf. Fig. 1(b)):

$$Q_{g,eb} = f(N_{eng}, \Gamma) \tag{2}$$

On the other hand, the heat transfer to the coolant originates mainly from conduction through the area A_{eb}, and thus can be expressed as:

$$Q_{eb,c} = h_c A_{eb}\left(T_{eb} - \frac{T_{c,i} + T_{c,o}}{2}\right), \tag{3}$$

where an average value between the inlet and outlet flow temperatures is used to account for the distributed nature of the flow temperature.

In addition, the heat transfer coefficient h_c can be expressed by phenomenological laws (see for example the Colburn analogy (Bergman and Incropera, 2011)). In our case the following relation is used:

$$h_c A_{eb} = (hA)_{ref}\left(\frac{\dot{m}_{c,e}}{\dot{m}_{ref}}\right)^{0.75} \tag{4}$$

Coolant thermal balance. Following similar arguments, a heat balance equation gives:

$$\dot{T}_{c,o} = \frac{Q_{eb,c} - \Delta Q_c}{m_c c_c} \tag{5}$$

where ΔQ_c represents the heat flow due to the temperature difference at the input and the output of the engine. It can be expressed as:

$$\Delta Q_c = c_c \dot{m}_{c,e}(T_{c,o} - T_{c,i}) \tag{6}$$

Final second-order model. By combining these equations, we finally get the following second order system:

$$\Leftrightarrow \begin{cases} \dot{T}_{eb} = \dfrac{h_c(\dot{m}_{c,e})A_{eb}}{m_{eb}c_{eb}}\left(\dfrac{T_{c,o}}{2} - T_{eb}\right) \\ \qquad + \dfrac{Q_{g,eb}}{m_w c_{eb}} + \dfrac{h_c(\dot{m}_{c,e})A_{eb}}{m_{eb}c_{eb}}\dfrac{T_{c,i}}{2} \\ \dot{T}_{c,o} = \left(-\dfrac{h_c(\dot{m}_{c,e})A_{eb}}{2m_c c_c} - \dfrac{\dot{m}_{c,e}}{m_c}\right)T_{c,o} \\ \qquad + \dfrac{h_c(\dot{m}_{c,e})A_{eb}}{m_c c_c}T_{eb} \\ \qquad + \left(\dfrac{\dot{m}_{c,e}}{m_c} - \dfrac{h_c(\dot{m}_{c,e})A_{eb}}{2m_c c_c}\right)T_{c,i} \end{cases} \tag{7}$$

in which h_c is defined through (4).

It is worth noting that, in the sequel, it is assumed that the following variables are known (measured or estimated): N_{eng}; Γ; $T_{c,i}$ and $T_{c,o}$.

2.2 Flow modeling

Since the water pump is mechanically connected to the engine, its flow is a function of the engine speed. In order to simplify the model, we will use a crude approximation of this relation by assuming that:

$$\dot{m}_c = \alpha N_{pump}, \qquad \alpha \in \mathrm{R}^+ \tag{8}$$

For more detailed pump models see (Isermann, 2014).

As the pump speed is not measured but the engine one is, the following relation is also considered:

$$N_{pump} = r N_{eng}, \qquad r \in \mathrm{R}^+ \tag{9}$$

Finally, a part of the coolant recirculated by the water pump actually flows through the oil cooler instead of the engine. This is represented by a simplified proportional relation between the global mass flow rate and the engine block one:

$$\dot{m}_{c,e} = \beta \dot{m}_c, \qquad \beta \in [0; 1] \tag{10}$$

Plugging together (8)-(10), we have the simple relation:

$$\dot{m}_{c,e} = \sigma N_{eng}, \qquad \sigma \in \mathrm{R}^+ \tag{11}$$

in which $\sigma = \alpha \times \beta \times r$ is a constant [1].

2.3 Model validation

To validate this model, it is compared with one built with GT-SUITE [2]. This software, developed by Gamma Technology, consists in a set of simulation libraries for analyzing the engine behavior and is largely used in the automotive industry. As it enables to obtain a high-fidelity simulation, this model will be the reference one in the sequel.

For comparison purposes, the same scenario is used for the simplified model and the GT-SUITE one. It consists of the engine speed and load torque profiles presented in Fig. 2(a).

Under these conditions, the results obtained from GT-SUITE and from the developed model are given in Fig. 2(b).

It can be observed that the temperatures recovered from the simplified model match almost perfectly the reference ones. This justifies the use of the simplified model to design observers.

2.4 Fault diagnosis problem statement

The belt tensioner ensures power transmission between the engine and all the other components connected to the belt. A malfunction on the belt tensioner will affect the transmission ratio r in (9) which, in turn, will affect the mass flow rate in (8). Thus, from the cooling system (4), (7), (11) point of view, this malfunction will affect the nominal mass flow rate through a change of the parameter σ in (11). Note that this change will thus also affect the heat transfer coefficient h_c which depends on $\dot{m}_{c,e}$ through (4).

The paper objective is then to estimate the parameter σ to provide an indication of the belt tensioner's health.

3. OBSERVER-BASED FAULT ESTIMATION

To evaluate in real time the degradation of the transmission, observers have been designed and implemented to estimate the parameter σ which is considered to be constant (or slow-varying). Two types of observer are considered in the sequel. The first one is an adaptive observer and then an extended Kalman filter.

3.1 Adaptive observer

The adaptive observer design follows the method developed in (Besançon et al., 2006) and (Zhang and Clavel, 2001). Such an observer both estimates the state and unknown constant parameters involved in the dynamical equation. The system must be affine in the state and parameter vector as:

$$\begin{aligned} \dot{x} &= A(u,y)x + \varphi(u,y) + \Phi(u,y)\theta \\ y &= Cx \end{aligned} \tag{12}$$

where x, u, y classically denote the state, the input and the measured output vectors respectively and θ a vector of unknown constant parameters. The elements of the matrices $A(u,y)$ and $\Phi(u,y)$ and of the vector $\varphi(u,y)$ are assumed to be continuous and uniformly bounded functions.

If a persistent exciting condition is verified, i.e, if there exist positive constants $\alpha_{1,2}$, $\beta_{1,2}$, $T_{1,2}$ and some bounded symmetric positive definite matrix Σ such that, for all t, the following inequalities hold:

$$\alpha_1 I \leq \int_t^{t+T_1} \Lambda^T(\tau)C^T\Sigma(\tau)C\Lambda(\tau).d\tau \leq \beta_1 I \tag{13}$$

and

$$\alpha_2 I \leq \int_t^{t+T_2} \Psi^T(t,\tau)C^T\Sigma(\tau)C\Psi(t,\tau).d\tau \leq \beta_2 I \tag{14}$$

where Ψ is the transition matrix of the system $\dot{x} = A(u,y)x$, $y = Cx$, then, according to (Besançon et al., 2006) and (Zhang and Clavel, 2001), the following system is an exponential adaptive observer for the nonlinear system (12),

$$\begin{aligned} \dot{\hat{x}} &= A(u,y)\hat{x} + \varphi(u,y) + \Phi(u,y)\hat{\theta} \\ &\quad + \{\Lambda S_\theta^{-1}\Lambda^T C^T + S_x^{-1}C^T\}\Sigma(y - C\hat{x}) \\ \dot{\hat{\theta}} &= S_\theta^{-1}\Lambda^T C^T \Sigma(y - C\hat{x}) \\ \dot{\Lambda} &= \{A(u,y) - S_x^{-1}C^T\Sigma C\}\Lambda + \Phi(u,y) \\ \dot{S_x} &= -\rho_x S_x - A(y,u)^T S_x - S_x A(u,y) + C^T\Sigma C \\ \dot{S_\theta} &= -\rho_\theta S_\theta + \Lambda^T C^T \Sigma C \Lambda, \qquad S_x(0),\, S_\theta(0) > 0 \end{aligned} \tag{15}$$

[1] This approximation is verified if the resistance coefficient of the cooling system is constant, that is, when the thermostat position is fixed (after engine start-up).

[2] www.gtisoft.com

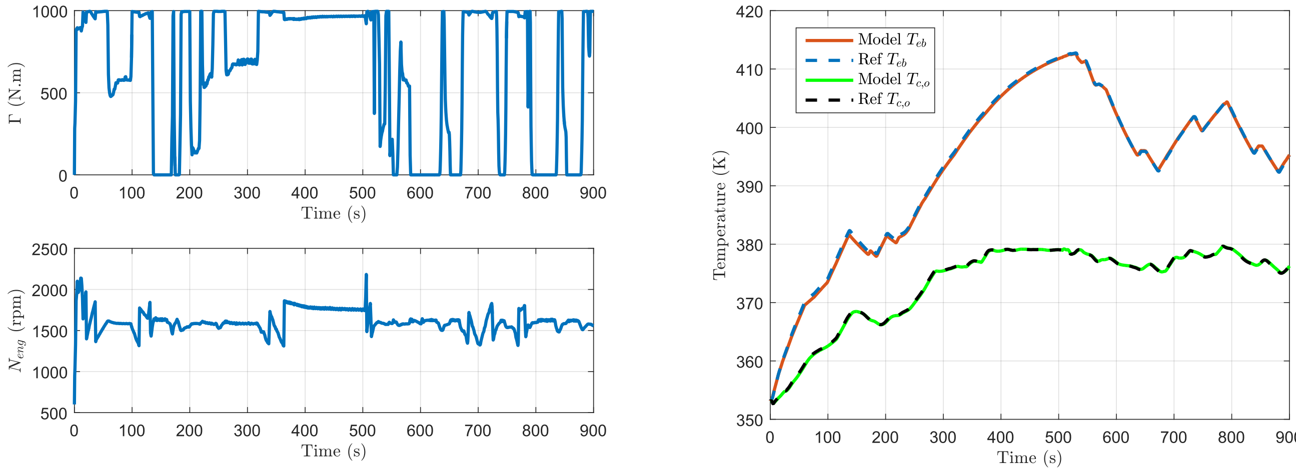

(a) (b)

Fig. 2. (a) Torque and engine speed profiles (b) Comparison between the reference and the simplified model

where ρ_x and ρ_θ are tunable parameters. It is worth noting that Λ, S_x and S_θ are time-varying observer gains.

In order to apply this observer to the cooling system (4), (7), (11) let us note:

$$\begin{aligned} \theta_1 &= h_c A_{eb} \qquad \theta_2 = \dot{m}_{ce} c_c \\ a_1 &= m_{eb} c_{eb} \qquad a_2 = m_c c_c \end{aligned} \tag{16}$$

Introducing intuitively $z = [T_{eb} \;\; T_{c,o}]^T$; $u = [Q_{g,eb} \; T_{c,i}]^T$, one obtains the following equivalent state-space representation:

$$\begin{aligned} \dot{z} &= \begin{bmatrix} -\dfrac{\theta_1}{a_1} & \dfrac{\theta_1}{2a_1} \\ \dfrac{\theta_1}{a_2} & -\dfrac{\theta_1 + 2\theta_2}{2a_2} \end{bmatrix} z + \begin{bmatrix} \dfrac{1}{a_1} & \dfrac{\theta_1}{2a_1} \\ 0 & \dfrac{\theta_2}{a_2} - \dfrac{\theta_1}{2a_2} \end{bmatrix} u \\ y &= [0 \;\; 1]\, z \end{aligned} \tag{17}$$

which unfortunately does not fit the formalism of (12) as it introduces bilinear terms $\theta_1 z_1$ in which z_1 is not measured. To solve this problem, (17) is turned into its companion form. With this aim in view, the following coordinate transformation is used:

$$x = \begin{bmatrix} \dfrac{\theta_1}{a_2} & \dfrac{\theta_1}{a_1} \\ 0 & 1 \end{bmatrix} z \tag{18}$$

This leads to:

$$\begin{aligned} \dot{x} &= \begin{bmatrix} 0 & 0 \\ 1 & 0 \end{bmatrix} x \\ &+ \begin{bmatrix} \dfrac{u_2 - x_2}{a_1 a_2} & \dfrac{u_1}{a_1 a_2} & 0 \\ 0 & -\dfrac{x_2}{a_1} - \dfrac{x_2 + u_2}{2a_2} & \dfrac{u_2 - x_2}{a_2} \end{bmatrix} \theta \\ y &= [0 \;\; 1]\, x \end{aligned} \tag{19}$$

where $\theta = [\theta_1\theta_2 \;\; \theta_1 \;\; \theta_2]^T$. Therefore (19) satisfies the required form (12).

To estimate the parameter σ, it is important to note that, by using (4) and (11):

$$\begin{aligned} \theta_1 &= (hA)_{ref} \left(\frac{N_{eng}}{\dot{m}_{ref}}\right)^{0.75} \sigma^{0.75} \triangleq f(N_{eng})\sigma^{0.75} \\ \theta_2 &= c_c N_{eng} \sigma \triangleq g(N_{eng})\sigma \end{aligned} \tag{20}$$

Thus, if the vector θ is divided term by term by:

$$[f(N_{eng})g(N_{eng}) \;\; f(N_{eng}) \;\; g(N_{eng})]^T,$$

the AO can provide an estimation of $\left[\sigma^{1.75} \;\; \sigma^{0.75} \;\; \sigma\right]^T$.

3.2 *Extended Kalman filter*

For the ease of comparison, a classical EKF is also designed. Since σ is constant, the dynamic $\dot{\sigma} = 0$ is added to the system (7) to obtain a third order system described by:

$$\begin{aligned} \dot{x}(t) &= f(x(t), u(t)) \\ y &= Cx(t) \end{aligned} \tag{21}$$

with $x = [\sigma \;\; T_{eb} \;\; T_{c,o}]^T$; $u = [Q_{g,eb} \;\; T_{c,i}]^T$ and $C = [0 \;\; 0 \;\; 1]$.

Note that assuming σ constant is not restrictive since it corresponds to the needed assumption in adaptive observer design for parameter estimation.

Without entering into well-known details (see for instance Chui and Chen (2009) for the theory and Boussak (2005); Janiszewski (2006) for EKF applications), the following algorithm is used to estimate the states of (21):

$$\dot{\hat{x}}(t) = f(\hat{x}(t), u(t)) + K(t)(y(t) - C\hat{x}(t)) \tag{22}$$

where the optimum gain $K(t)$ satisfies the following equations:

$$
\begin{aligned}
K(t) &= P(t)C^T R^{-1} \\
\dot{P}(t) &= F(t)P(t) + P(t)F(t)^T - K(t)CP(t) + Q \\
P(0) &= P_0 = P_0^T \\
F(t) &= \frac{\partial f}{\partial x}(\hat{x}(t), u(t))
\end{aligned}
\tag{23}
$$

where Q and R are the covariance matrices of the system and measurement respectively.

4. SIMULATION RESULTS

To compare the merits of the two methods previously presented, we set them in various contexts on the reference model developed with GT-SUITE. The following initial conditions and tuning parameters (chosen to get a trade-off between convergence speed and noise attenuation) have been used in all cases.

Concerning the adaptive observer (15), (19):

- $\rho_x = \rho_\theta = 75 \times 10^{-3}$
- $\hat{\theta}(0) = [f(N_{eng}(0))g(N_{eng}(0))0.002^{1.75}$ $f(N_{eng}(0))0.002^{0.75}$ $g(N_{eng}(0))0.002]^T$, $S_x(0) = I_2$, $S_\theta(0) = I_3$, $\Lambda(0) = \mathcal{O}_{2,3}$, $\hat{x}(0) = [29 \;\; 353.15]^T$

Concerning the EKF (22), (23):

- $Q = 100 \times I_3$, $R = 10^8$
- $\hat{x}(0) = [0.002 \;\; 353.15 \;\; 353.15]^T$, $P(0) = I_3$

It is worth noting that the initial conditions provided to the two observers are consistent with each other.

4.1 Fault scenario

In Section 2.4, it has been established that σ is a function of the ratio r defined in (9). To simulate a fault on σ let us consider the following evolution of r:

$$
r(t) = \begin{cases} 1.4 & \text{for } t < 500 \text{ s} \\ 0.7 & \text{for } t \geq 500 \text{ s} \end{cases} \tag{24}
$$

The fault is implemented in GT-SUITE through the operating point N_{pump} provided to the water pump. Data are then collected to feed the developed observers. Then, following (11), the real σ is computed as: $\sigma_{real} = \dot{m}_{c,e}/N_{eng}$. It is depicted with the dashed plot in the Fig. 3, 5 and 6. Note also that the AO estimates a vector of three coherent parameters but only the third term will be ploted in the sequel.

4.2 First simulation case: constant engine speed and torque

First, let us consider the simple case of a given constant operating point:

$$N_{eng} = 1600 \text{ rpm}, \;\; \Gamma = 816 \text{ N.m}$$

The results corresponding to this case are given in Fig. 3. One can observe that the EKF estimates the value of the parameter σ with a short settling time. On the other hand, the estimation of σ provided by the AO introduces a bias. This can be explained from the fact that the condition of persistent excitation (13) is not fulfilled. Indeed, if the speed and the torque are constant, it means that the heat flow $Q_{g,eb}$ described by (2) is constant.

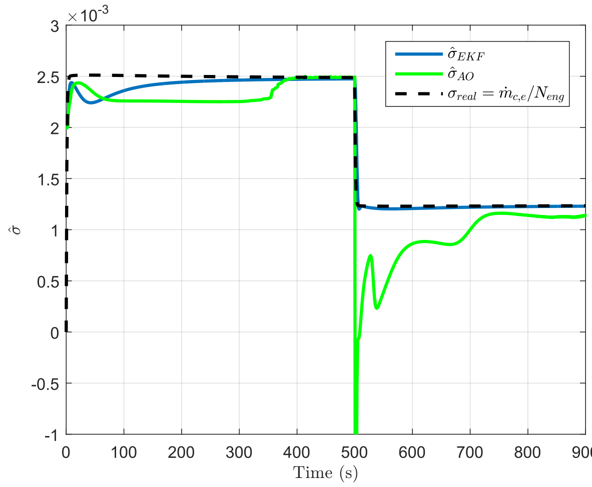

Fig. 3. Estimation results obtained in the first case

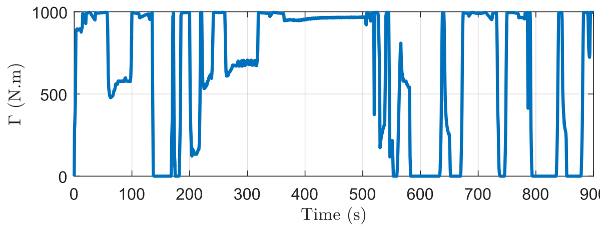

Fig. 4. Torque profile in the second case

Thus the variable u_1 in (19) is not excited and so the observer cannot converge. Consequently, for this scenario, the adaptive observer is not suitable as it suffers from significant limitations.

4.3 Second simulation case: constant engine speed and time-varying torque

To guarantee the persistent excitation condition, the torque profile is changed into the one depicted in the Fig. 4. The engine speed is still equal to 1600 rpm.

The obtained results are presented in Fig. 5. The persistent excitation is now fulfilled, and one can observe that both observers converge and correctly estimate the value of the parameter σ. However, the AO has a significant overshoot which may be unsuitable for fault detection.

4.4 Third simulation case: realistic profiles

Until now, the engine speed was kept constant in order to respect the assumption that the vector θ is constant. Indeed, if N_{eng} is varying, so are the parameters θ_1 and θ_2 in (20). To evaluate the performance of the EKF in a more practically meaningful context, let us consider a third case where torque and speed engine profiles are time-varying. Besides, a white Gaussian noise with a variance of 0.05 is added to the measures $T_{c,o}$ and $T_{c,i}$. The considered profiles are the ones given in Fig. 2(a). Corresponding simulations results are depicted in Fig. 6. One can observe that, even in a noisy realistic case, the estimation capabilities remain similar to the ones obtained in the previous case.

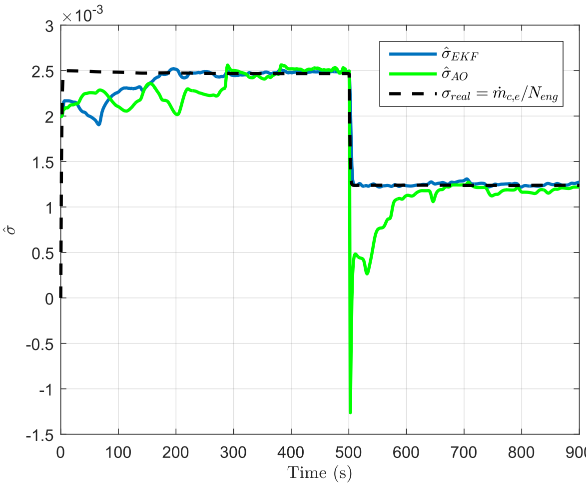

Fig. 5. Estimation results obtained in the second case

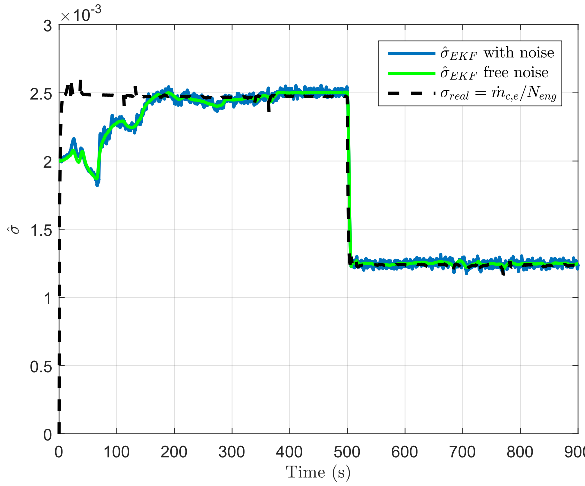

Fig. 6. Estimation results obtained in the third case

5. CONCLUSION

In this paper we have proposed a method to estimate the performance degradation of a belt tensioner from the cooling system point of view. A simplified control-oriented model has been developed and validated with a more complex model developed in GT-SUITE. The model was then used to design an adaptive observer and an Extended Kalman Filter.

It has been established in Section 5 that the EKF has better transient performance than the AO to estimate the parameter σ. Besides, the EKF estimation requires fewer assumptions but it is well known that its convergence is just local and may have numerical instability (Verhaegen and Van Dooren, 1986). On the other hand, the AO only converges if the engine speed is constant, with sufficient excitation on $Q_{g,eb}$. This condition is, in practice, difficult to obtain, as it implies that the rotation must be constant while providing a variable torque (Fig. 4). However it is less conservative than the EKF, in the sense that, it does not estimate only σ but also the coolant heat transfer coefficient h_c and the coolant mass flow rate $\dot{m}_{c,e}$ via θ_1 and θ_2 in the representation (19) where faults can occur. Indeed, in (Astorga-Zaragoza et al., 2008) the authors estimate the heat transfer coefficient in order to prevent a degradation.

We may also conclude that a single observer is not enough to detect and isolate the fault on the belt tensioner. In fact, as said before, a fault may also occur in other components of the cooling system. For example, a fault on the coolant mass flow rate, as a leak, will affect σ. To overcome this problem, the monitoring of all the other systems driven by the belt. This is a direction of ongoing work.

REFERENCES

Astorga-Zaragoza, C.M., Alvarado-Martínez, V.M., Zavala-Río, A., Méndez-Ocaña, R.M., and Guerrero-Ramírez, G.V. (2008). Observer-based monitoring of heat exchangers. *ISA Transactions*, 47(1), 15–24.

Bergman, T.L. and Incropera, F.P. (eds.) (2011). *Fundamentals of heat and mass transfer*. Wiley, Hoboken, NJ, 7th ed edition.

Besançon, G., De León-Morales, J., and Huerta-Guevara, O. (2006). On adaptive observers for state affine systems. *International Journal of Control*, 79(6), 581–591.

Boussak, M. (2005). Implementation and Experimental Investigation of Sensorless Speed Control With Initial Rotor Position Estimation for Interior Permanent Magnet Synchronous Motor Drive. *IEEE Transactions on Power Electronics*, 20(6), 1413–1422.

Chen, J. and Patton, R.J. (1999). *Robust Model-Based Fault Diagnosis for Dynamic Systems*. Springer US, Boston, MA.

Chui, C.K. and Chen, G. (2009). *Kalman filtering: with real-time applications*. Springer, Berlin, 4th ed edition.

Cortona, E., Onder, C.H., and Guzzella, L. (2002). Engine thermomanagement with electrical components for fuel consumption reduction. *International Journal of Engine Research*, 3(3), 157–170.

Ding, S.X. (2008). *Model-based fault diagnosis techniques: design schemes, algorithms, and tools*. Springer, Berlin.

Hwang, I., Kim, S., Kim, Y., and Seah, C.E. (2010). A Survey of Fault Detection, Isolation, and Reconfiguration Methods. *IEEE Transactions on Control Systems Technology*, 18(3), 636–653.

Isermann, R. (2014). *Engine modeling and control: modeling and electronic management of internal combustion engines*. Springer, Heidelberg.

Janiszewski, D. (2006). Extended Kalman Filter Based Speed Sensorless PMSM Control with Load Reconstruction. 1465–1468. IEEE.

Tami, R., Boutat, D., and Zheng, G. (2014). Nonlinear observer for the PM synchronous motor. 4133–4138. IEEE.

Verhaegen, M. and Van Dooren, P. (1986). Numerical aspects of different Kalman filter implementations. *IEEE Transactions on Automatic Control*, 31(10), 907–917.

Zhang, Q. and Clavel, A. (2001). Adaptive observer with exponential forgetting factor for linear time varying systems. In *Decision and Control, 2001. Proceedings of the 40th IEEE Conference on*, volume 4, 3886–3891. IEEE.